Research Article

In Silico Analysis of the Antigastritis Activity of Gedi (*Abelmoschus manihot*) Flower Flavonoids on H₂ Receptor

Gregorius Giani Adikila [1]

Yuanita Amalia Hariyanto [1]

Trina Ekawati Tallei [2]

Elly Juliana Suoth [1]

Sri Sudewi [1]

Fatimawali [3*]

[1] Department of Pharmacy, Universitas Sam Ratulangi, Manado, North Sulawesi, Indonesia
[2] Department of Biology, Universitas Sam Ratulangi, Manado, North Sulawesi, Indonesia
[3] Department of Medical Education, Universitas Sam Ratulangi, Manado, North Sulawesi, Indonesia

*email: fatimawali@unsrat.ac.id; phone: +62431820300

Abstract

Gastritis remains a highly prevalent health concern in Indonesia, underscoring a continuous demand for innovative therapeutic interventions. The flower of *Abelmoschus manihot*, commonly known as Gedi, has garnered interest for its potential antigastritis properties, specifically as an H₂ antagonist, attributed to its rich flavonoid content. This study aimed to rigorously evaluate the H₂ antagonist potential of *A. manihot* flowers using an *in silico* approach. Our research methodology involved assessing the physicochemical and pharmacokinetic profiles, alongside molecular docking simulations, of ten prominent flavonoid ligands identified in *A. manihot* flowers: quercetin, myricetin, myricetin-3-O-glucoside, myricetin-3'-O-glucoside, quercetin-3'-O-glucoside, hibifolin, isoquercetin, hyperoside, quercetin-3-O-robinobioside, and rutin. The analysis of physicochemical and pharmacokinetic properties encompassed Lipinski's Rule of Five and comprehensive ADMET predictions. Molecular docking simulations focused on evaluating binding energies and interactions with crucial H₂ receptor residues: Asp98, Asp186, Val99, and Phe254. Among the ligands being assessed, quercetin demonstrated the most favorable physicochemical-pharmacokinetic characteristics and exhibited superior binding affinities and interactions in the molecular docking analysis. These findings collectively suggest that *A. manihot* flower holds significant promise as a natural source for antigastritis agents, specifically through its potential H₂ antagonist activity, with quercetin emerging as a key contributing compound.

INTRODUCTION

Gastritis, an inflammatory condition of the stomach lining, is a highly prevalent gastrointestinal disorder. The World Health Organization's (WHO) 2023 World Health Statistics report estimates that approximately 10% of the global population has experienced this condition at some point in their lives[1]. In Southeast Asia, Indonesia faces a particularly high prevalence rate of around 40.8%, highlighting a significant public health burden and the importance of continued development of traditional remedies using natural ingredients[2].

The Gedi (*Abelmoschus manihot* L.) plant is a notable species in Indonesia with a long history of empirical use for various ailments. Specifically, the leaves have been traditionally used by communities in North Sulawesi to treat ulcers[3]. Beyond the leaves, the plant's flowers have also shown promising antigastritis activity in *in vivo* studies, demonstrating their ability to prevent acid reflux[4]. This therapeutic effect is linked to the flowers' rich phytochemical composition, which is abundant in flavonoids such as quercetin, myricetin, hyperoside, and hibifolin. Quantitatively, hyperoside and hibifolin are the most prevalent flavonoids, with concentrations of 33,986.66 µg/g and 10,006.27 µg/g, respectively[5]. These flavonoids are known

to possess gastroprotective properties and are thought to inhibit gastric acid secretion, with some acting similarly to H_2 receptor antagonists[6,7].

To further investigate the therapeutic potential of *A. manihot* flowers, this study employs an *in silico* approach, specifically molecular docking. This computational method allows for the analysis of chemical interactions between the plant's compounds and the histamine H_2 receptor. The H_2 receptor is a highly effective target for anti-ulcer drug development due to its selective action on gastric parietal cells, which makes it a more precise and consistent target compared to the less specific M_3 and CCK-B receptors[8]. Furthermore, inhibiting the H_2 receptor typically results in fewer side effects than inhibiting the widely distributed M_3 receptors. This clinical and pharmacological advantage solidifies the H_2 receptor's status as a key target for anti-ulcer drug candidates[9]. The continued use of the H_2 receptor as a primary target in recent studies[10], along with the enduring relevance of molecular docking as a computational method for drug research, supports our methodological choice. Thus, by utilizing molecular docking, this study aims to assess the potential of *A. manihot* flowers as a natural source for gastritis treatment.

MATERIALS AND METHODS

Materials

This study utilized both receptor and ligand files for molecular docking analysis. The histamine H_2 receptor protein structure was sourced from the Research Collaboratory for Structural Bioinformatics Protein Data Bank (RCSB PDB), with the specific entry identified as PDB: 7UL3. As a positive control ligand, ranitidine (CID: 3001055) was obtained from the PubChem database. The nine test ligands—quercetin (CID: 5280343), myricetin (CID: 5281672), myricetin 3-O-glucoside (CID: 5318606), myricetin 3'-O-glucoside (CID: 12302392), quercetin 3'-O-glucoside (CID: 5748594), hibifolin (CID: 5490334), isoquercetin (CID: 5280804), hyperoside (CID: 5281643), quercetin-3-O-robinobioside (CID: 10371536), and rutin (CID: 5280805)—were also acquired from the PubChem database.

Methods

Preparation of protein and ligands

To prepare for the molecular docking simulation, both the receptor and ligand structures were pre-processed. The H_2 receptor protein was obtained as a PDB file from the RCSB PDB database. Its native ligand was then separated from the receptor using BIOVIA Discovery Studio, and the cleaned receptor was saved in PDB format for subsequent use. The control ligand, ranitidine, along with the 10 test ligands, was downloaded from PubChem as 3D structures in SDF file format. All ligand files were converted to PDB format using the Open Babel program.

For the docking process, all molecules—the prepared receptor, its native ligand, the control ligand, and the test ligands—underwent a crucial pretreatment step in AutoDockTools. During this step, charges and hydrogen atoms were added to each molecule to ensure accurate interaction modeling. Finally, all pretreated molecules were saved in PDBQT format, which is the required input format for AutoDock. This meticulous preparation of both the receptor and ligands was essential for the integrity and reliability of the molecular docking simulations.

Analysis of physicochemical and pharmacokinetic properties

The physicochemical properties, ADMET (absorption, distribution, metabolism, excretion, and toxicity) of the test ligands were analyzed using established computational tools. Lipinski's rule of five and other key physicochemical properties were evaluated with the SwissADME web server. ADME and toxicity profiles were assessed using the pkCSM online platform. For both analyses, the SMILES (Simplified Molecular-Input Line-Entry System) notation for each compound was required. These SMILES strings were generated by converting the corresponding PDB files of the ligands using the OpenBabel program. This integrated approach allowed for a comprehensive *in silico* prediction of the compounds' drug-likeness, bioavailability, and safety profiles[11].

Molecular docking

Molecular docking was performed using the GNINA software to evaluate the binding affinity of the test ligands to the histamine H_2 receptor. All molecular structures, including the receptor (PDB: 7UL3), the native ligand, the positive control ligand (ranitidine), and the nine test ligands, were uploaded to the GNINA platform. First, the native ligand was redocked

into the receptor's active site to validate the docking protocol. A grid box was manually defined around the binding site, and its dimensions were optimized until a root-mean-square deviation (RMSD) value of less than 2 Å was achieved, indicating a reliable and reproducible docking pose. Once the optimal grid box was established, molecular docking was performed for the positive control and all test ligands.

The docking results, in the form of SDF files, were then downloaded and analyzed using BIOVIA Discovery Studio. The best molecular pose for each ligand was selected based on the lowest binding affinity, signifying the strongest predicted interaction with the receptor. Each of these optimal poses was then saved in PDB format, resulting in a total of 12 molecules (one native, one control, and ten test ligands). Finally, the interactions between the ligands and the receptor were visualized using BIOVIA Discovery Studio to provide a detailed understanding of the binding mechanisms.

Data analysis

The physicochemical properties of the ligands were analyzed using the SwissADME web server, with results assessed based on Lipinski's rule of five criteria. Pharmacokinetic properties were evaluated using both the SwissADME and pkCSM platforms, considering parameters such as absorption, distribution, metabolism, and excretion. The molecular docking results were analyzed by two primary criteria: binding energy and key amino acid interactions. To be considered a promising candidate, a ligand was required to have the lowest possible binding energy and form interactions with critical amino acid residues, specifically Asp98, Asp186, Val99, and Phe254, as identified in a previous study[12].

RESULTS AND DISCUSSION

The physicochemical properties of the ligands were evaluated for their adherence to Lipinski's rule of five, and the results are presented in **Table I**. This rule is a widely used guideline for assessing the oral bioavailability and drug-likeness of a compound based on its structural characteristics[13]. For this study, the SwissADME online tool was used, which specifies that a compound must satisfy at least three of the four core criteria to be considered compliant[14]. These criteria are molecular weight, logP, hydrogen bond donors, and hydrogen bond acceptors. A supplementary criterion, topological polar surface area or TPSA, also contributes to the assessment of a drug candidate's optimal bioavailability[13]. Our analysis revealed that of the ten ligands tested, only quercetin and myricetin met the criteria for Lipinski's rule of five compliance. Although myricetin did not meet the recommended TPSA threshold, it is still considered to be Lipinski's rule of five-compliant, as drug bioavailability is a complex property influenced by a multitude of ADMET factors beyond TPSA alone. The compliance of these two compounds suggests their potential for oral bioavailability and highlights their suitability as candidates for further *in vivo* and clinical investigation.

Table I.   Lipinski's rule of five on test ligands.

Parameters	Standard	Quercetin	Myricetin	Myricetin 3-O-glucoside	Myricetin 3'-O-glucoside	Quercetin 3'-O-glucoside
Mol. Weight (g/mol)	<500	302.24	318.24	480.38	480.38	464.38
H-bond donor	≤5	5	6	9	9	8
H-bond acceptor	≤10	7	8	13	13	12
LogP	<4.15	-0.56	-1.08	-3.07	-3.07	-2.59
TPSA (Å)	≤140	131.36	151.59	230.74	230.74	210.51
Interpretation		✓	✓	X	X	X
Parameters	**Standard**	**Hibifolin**	**Isoquercetin**	**Hyperoside**	**Quercetin 3-O-robinobioside**	**Rutin**
Mol. Weight (g/mol)	<500	494.36	464.38	464.38	610.52	610.52
H-bond donor	≤5	9	8	8	10	10
H-bond acceptor	≤10	13	12	12	16	16
LogP	<4.15	-3.08	-2.59	-2.59	-3.89	-3.89
TPSA (Å)	≤140	247.81	210.51	210.51	269.43	269.43
Interpretation		X	X	X	X	X

Note: ✓ = fulfill; **X** = Not fulfill

Pharmacokinetic analysis is essential for evaluating a compound's potential to become a safe and effective medicine. This analysis, encompassing absorption, distribution, metabolism, elimination, and toxicity, is summarized for the tested ligands in **Table II**. Regarding absorption, key metrics include LogS, gastrointestinal absorption (GI absorption), and P-glycoprotein

(P-gp) substrate status. LogS, which measures a compound's water solubility, is particularly important for drugs intended for the water-rich gastrointestinal environment[15]. High GI absorption indicates a compound's likelihood of being well-absorbed by the body[16], while P-gp substrate status suggests that the compound may be rapidly eliminated by this efflux pump[17]. Based on these criteria, the ligands were ranked in descending order of favorability: ranitidine, quercetin, myricetin, followed by the group of isoquercetin, hyperoside, and quercetin 3'-O-glucoside, then myricetin 3-O-glucoside and myricetin 3'-O-glucoside, and finally quercetin-3-O-robinobioside, rutin, and hibifolin.

For distribution, the volume of distribution and the fraction unbound were assessed. The volume of distribution indicates the extent to which a drug is distributed into tissues[18], while the fraction unbound represents the portion of the drug available to exert its pharmacological effect[19]. The ranking for distribution was determined by comparing the values to those of the control ligand, ranitidine, with the best-performing ligands being myricetin 3-O-glucoside, quercetin, ranitidine, myricetin 3'-O-glucoside, quercetin 3'-O-glucoside, myricetin, hibifolin, isoquercetin/hyperoside, and quercetin-3-O-robinobioside/rutin.

The metabolism of the compounds was primarily evaluated by their interaction with cytochrome P450 (CYP) enzymes, particularly those in the CYP1-3 family, which are responsible for metabolizing most drugs[20]. While inhibiting these enzymes can increase a drug's concentration and duration of action, it can also lead to toxicity[21]. Therefore, a balanced approach is needed. In this analysis, all ligands were deemed acceptable, with most test ligands showing no inhibitory effect on CYP enzymes, similar to ranitidine. Quercetin and myricetin, however, were found to inhibit several P450 enzymes. This inhibitory effect may be beneficial, as it could slow their metabolism, prolonging the activity of the small fraction of free drugs in the tissue.

In terms of elimination, we examined renal OCT2 substrate status, which relates to the clearance of cationic drugs[22], and total clearance, an indicator of a compound's elimination efficiency[23]. The optimal total clearance value was determined by comparing it with the reference value for H_2 antagonists. The most favorable ligands in this category were: ranitidine, isoquercetin/hyperoside, myricetin, hibifolin, quercetin, quercetin-3-O-robinobioside/rutin, myricetin-3'-O-glucoside, myricetin-3-O-glucoside, and quercetin-3'-O-glucoside.

Finally, the toxicity of the ligands was assessed by evaluating their potential for mutagenicity (Ames toxicity), hepatotoxicity, and hERG inhibition. The hERG gene is critical for heart function, and its inhibition can lead to fatal cardiac arrhythmias[24]. In this analysis, the safest ligands were found to be quercetin, myricetin, and hibifolin, which demonstrated a low risk of toxicity across the criteria assessed. Overall, these pharmacokinetic and toxicity profiles, when combined with the physicochemical properties and molecular docking results, provide a comprehensive assessment of the ligands' potential as drug candidates.

Molecular docking was performed on all native, control, and test ligands. To ensure the reliability of the docking method, a redocking validation was conducted by re-docking the native ligand to the receptor, as shown in **Figure 1**. This procedure validates the appropriateness of the chosen binding site by calculating RMSD value[25]. A low RMSD value, specifically one less than 2 Å, indicates that the docking method is of high quality and that the predicted binding pose closely matches the experimentally determined one[26].

The validation yielded an RMSD value of 1.67933 Å, which is well below the 2 Å threshold. This confirms the good quality and reliability of our molecular docking methodology. The optimal grid box parameters that produced this result were centered at coordinates x = 159.095, y = 164.736, and z = 200.326, with dimensions of x = 12, y = 10, and z = 6. Following validation, the binding interactions of the control and test ligands with the receptor were visualized using BIOVIA Discovery Studio, as presented in **Figure 2**.

The molecular interactions between ligands and the H_2 receptor are governed by a combination of non-covalent forces, including van der Waals, hydrogen bonds, π-system interactions, and hydrophobic bonds. Key amino acid residues critical for binding were identified as Asp98, Asp186, Val99, and Phe254. Asp98 serves as a primary binding residue, Asp186 provides stabilization to the binding complex, and Val99 and Phe254 mediate strong hydrophobic interactions. In the native ligand, a conventional hydrogen bond forms with Asp98, while Asp186 interacts via van der Waals forces, and Val99 binds through a π-alkyl bond[27]. Ranitidine, a control ligand, demonstrates distinct binding patterns. Its interaction with Asp98 is through a carbon-hydrogen bond, a type of covalent hydrogen bond. The interaction with Asp186 is mediated by weak van der Waals forces. Interestingly, while ranitidine interacts with Val99 and Phe254, these interactions are not classified as hydrophobic[28].
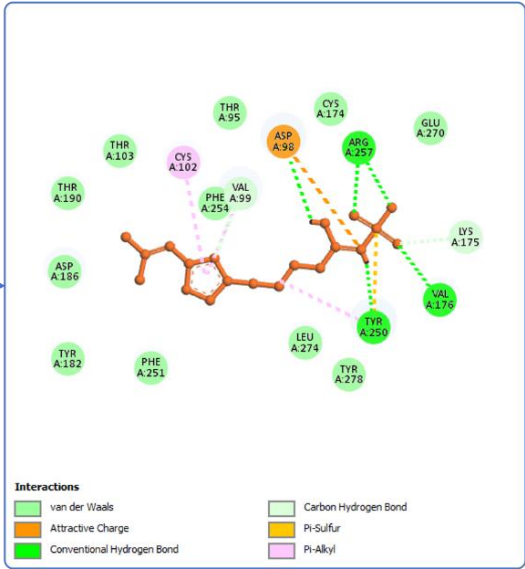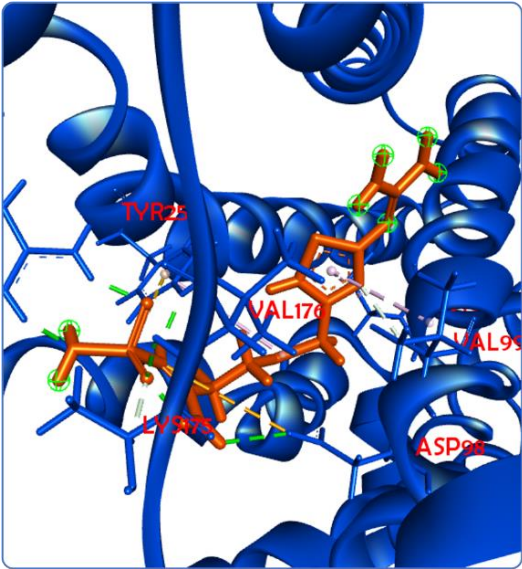
Table II.   ADMET properties analysis.

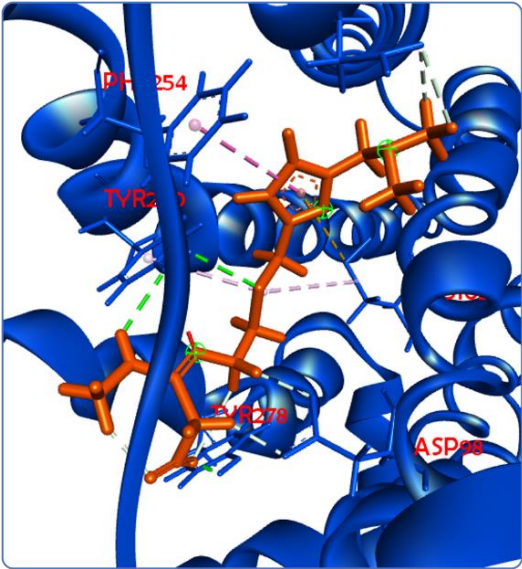| Parameters	Ranitidine	Quercetin	Myricetin	Myricetin 3-O-glucoside	Myricetin 3-O-glucoside	Quercetin 3-O-glucoside	Hibifolin	Isoquercetin	Hyperoside	Quercetin 3-O-robinobioside	Rutin
Absorption											
LogS[1]	-2.17	-3.91	-3.96	-4.41	-4.41	-4.35	-5.01	-4.35	-4.35	-4.87	-4.87
GI absorption[1]	High	High	Low	Low	Low	Low	Low	Low	Low	Low	Low
P-gp substrate[1]	Yes	No	No	No	No	No	Yes	No	No	Yes	Yes
Distribution											
Volume of distribution at steady state (VDss; L/kg)[2]	1.49	1.67	1.31	1.54	1.77	1.78	1.08	0.48	0.48	0.46	0.46
Fraction unbound[2]	0.705	0.061	0.053	0.265	0.279	0.238	0.273	0.143	0.143	0.274	0.274
Metabolism											
CYP1A2 inhibitor[1]	No	Yes	Yes	No	No	No	No	No	No	No	No
CYP2C19 inhibitor[1]	No	No	No	No	No	No	No	No	No	No	No
CYP2C9 inhibitor[1]	No	No	No	No	No	No	No	No	No	No	No
CYP2D6 inhibitor[1]	No	Yes	No	No	No	No	No	No	No	No	No
CYP3A4 inhibitor[1]	No	Yes	Yes	No	No	No	No	No	No	No	No
Elimination/excretion											
Renal OCT2 subtrate[2]	No	No	No	No	No	No	No	No	No	No	No
Total clearance (log mL/min/kg)[2]	7.09	4.6	4.12	0.41	0.45	0.39	4.11	5.47	5.47	1.08	1.08
Toxicity											
Ames toxicity[2]	No	No	No	No	No	No	No	Yes	Yes	Yes	Yes
Hepatotoxicity[2]	No	No	No	No	No	No	No	No	No	No	No
hERG I inhibitor[2]	No	No	No	No	No	No	No	No	No	No	No
hERG II inhibitor[2]	No	No	No	Yes	Yes	Yes	No	Yes	Yes	Yes	Yes

Note: [1] SwissADME; [2] pkCSM.

Among the test ligands, interactions with Asp98 were mediated by three types of bonds: hydrogen bonds, electrostatic bonds, and, in one case, an unfavorable steric bump. The strongest interactions with Asp98 were observed for quercetin 3'-O-glucoside and hyperoside, both forming two hydrogen bonds (conventional and carbon-hydrogen). Unlike covalent carbon-hydrogen bonds, conventional hydrogen bonds are non-covalent but are considered strong due to the high electronegativity of the participating atoms[29]. The electrostatic interaction, a π-anion bond, was also observed with Asp98. This non-covalent bond, formed between an electron-rich π-system and an anion, is generally weaker than a conventional hydrogen bond[30]. Notably, quercetin-3-O-robinobioside exhibited an unfavorable steric bump interaction, which can hinder the compound's optimal binding conformation[31]. At residue Asp186, most test ligands interacted via van der Waals forces. However, rutin formed a conventional hydrogen bond, making its interaction the strongest with this residue, while hibifolin's π-anion interaction made it the second strongest.

All test ligands, with the exception of quercetin-3-O-robinobioside, formed hydrophobic bonds with both Val99 and Phe254. These interactions included a variety of π-system-related bonds, such as π-alkyl, π-sigma, π-π stacked, and π-π T-shaped interactions. Since these are all non-covalent and involve π-systems, their individual bond strengths are considered comparable[29]. Therefore, the overall strength of hydrophobic binding is determined by the number of interactions. The binding affinities and specific interactions of the ligands are detailed in **Table III**.
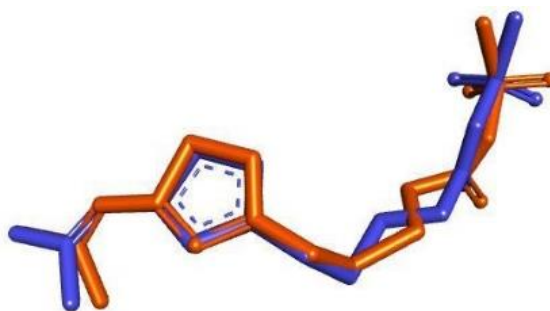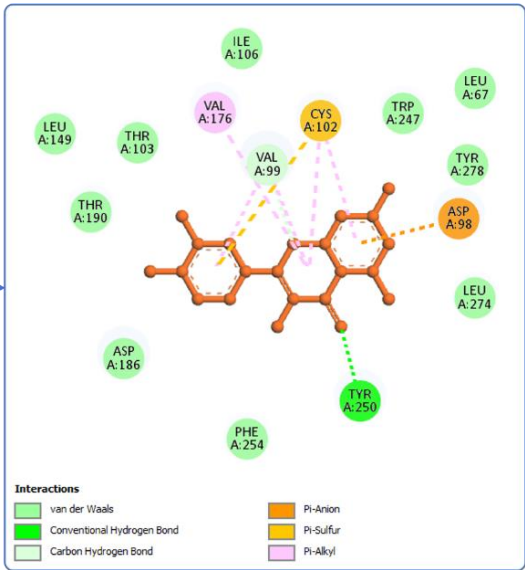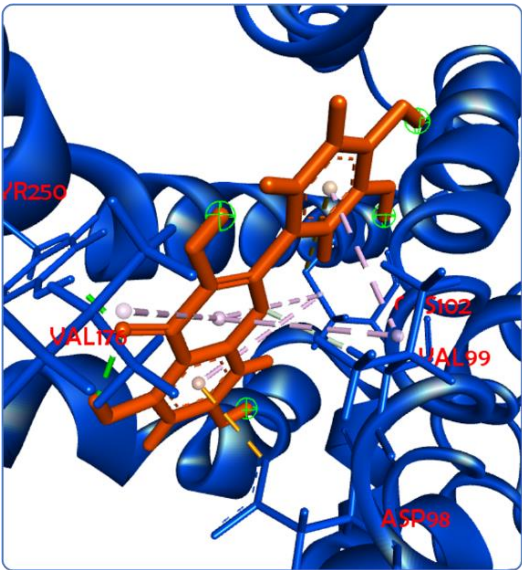

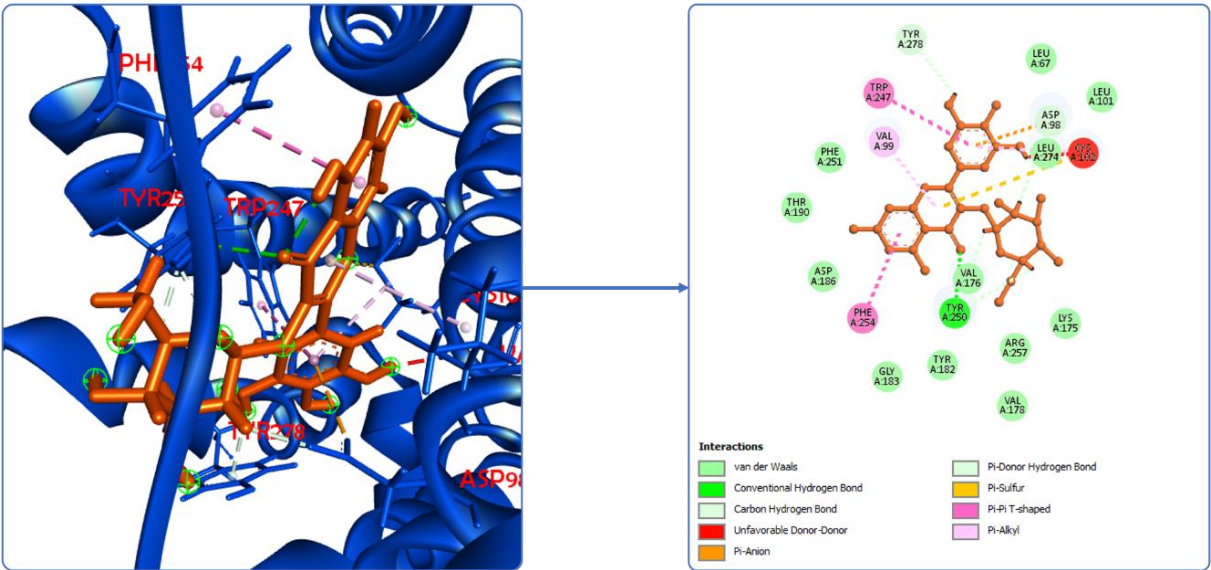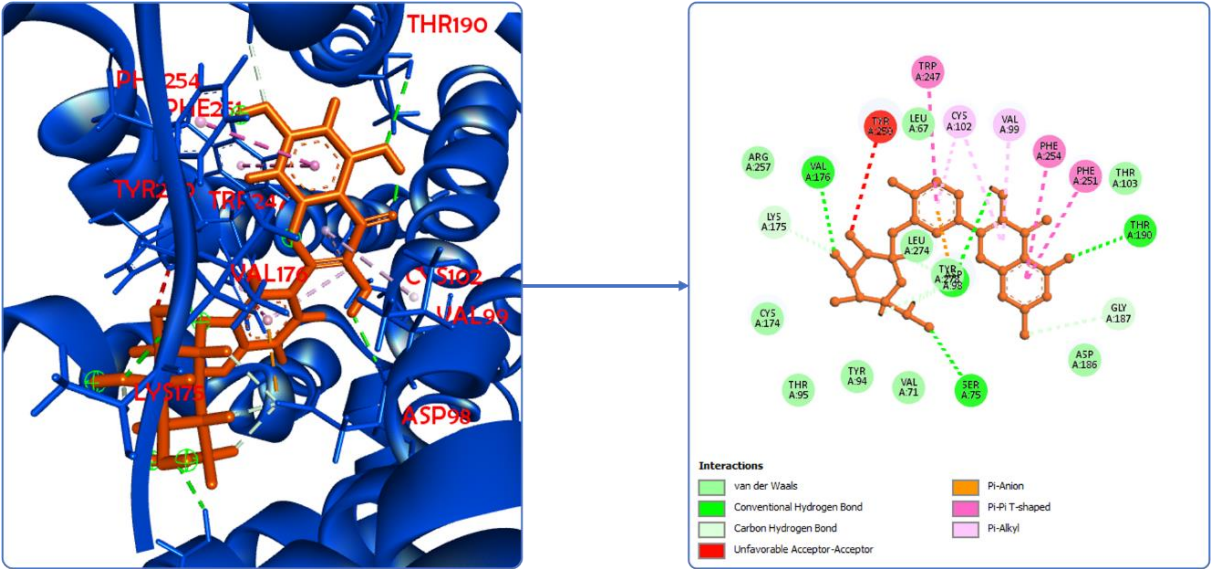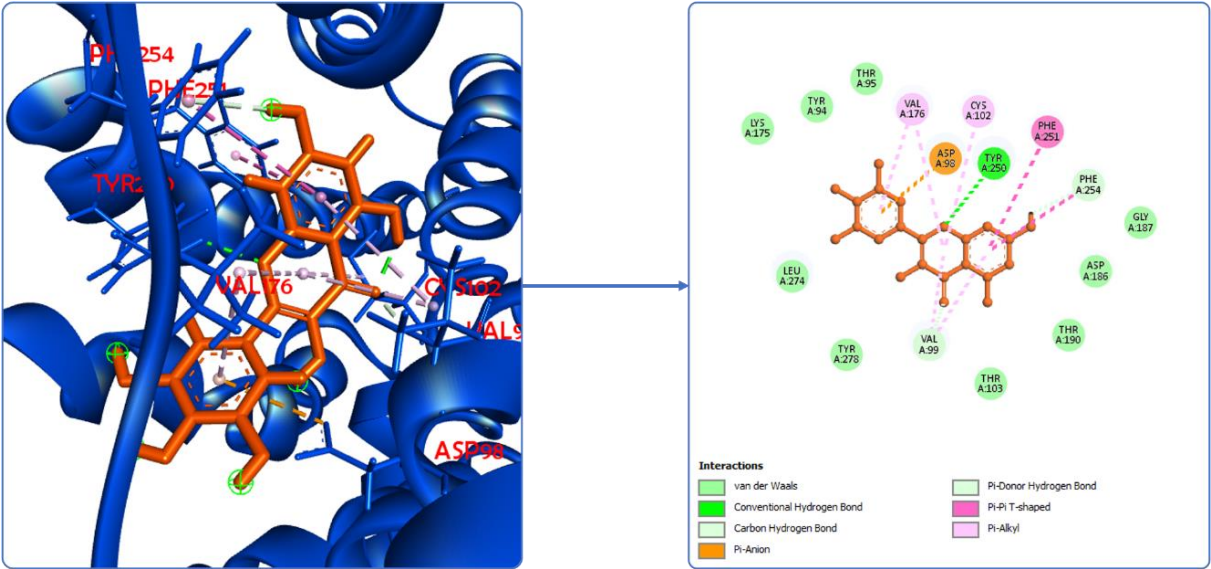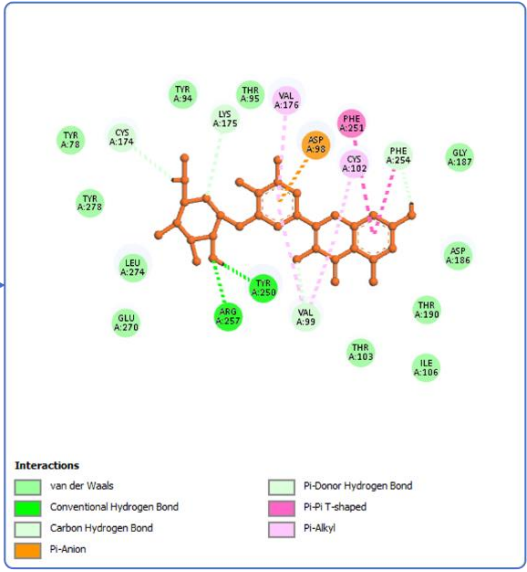**Figure 1.** Visualization of the native ligand before (blue) and after (orange) redocking.

a

b

c

d

e

f

g

h

i

Figure 2. 3D (left) and 2D (right) visualization of (**a**) native ligand, (**b**) ranitidine, (**c**) quercetin, (**d**) myricetin, (**e**) quercetin 3′-O-glucoside, (**f**) myricetin 3-O-glucoside, (**g**) myricetin 3′-O-glucoside, (**h**) hibifolin, (**i**) isoquercetin, (**j**) hyperoside, (**k**) quercetin 3-O-robinobioside, (**l**) rutin, and H₂ receptors.
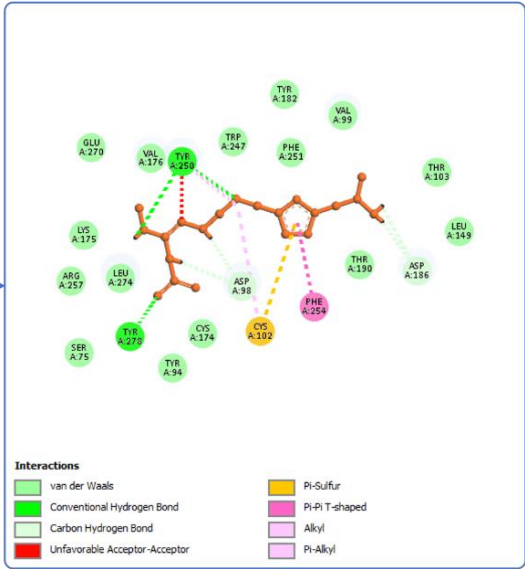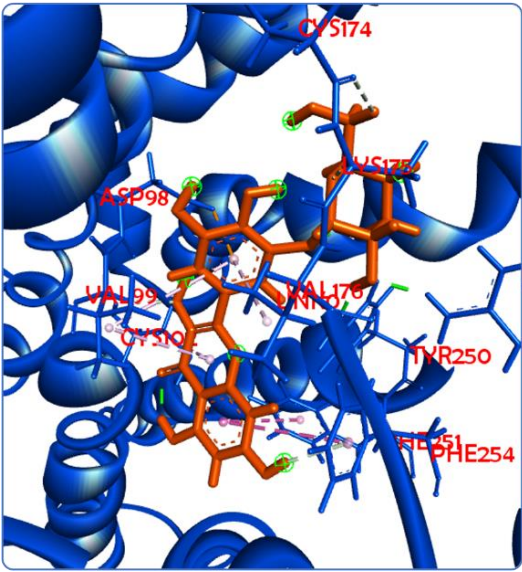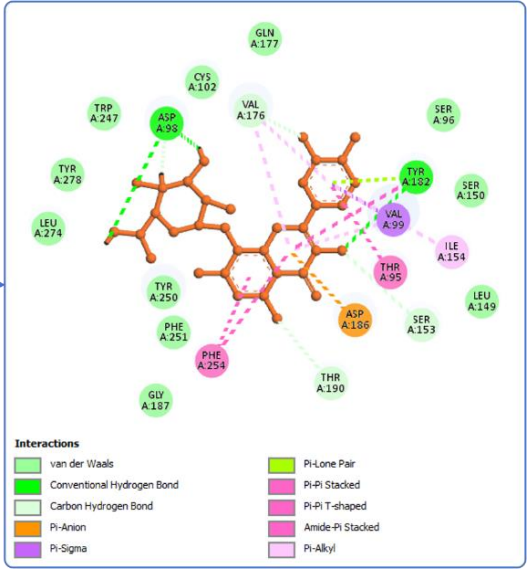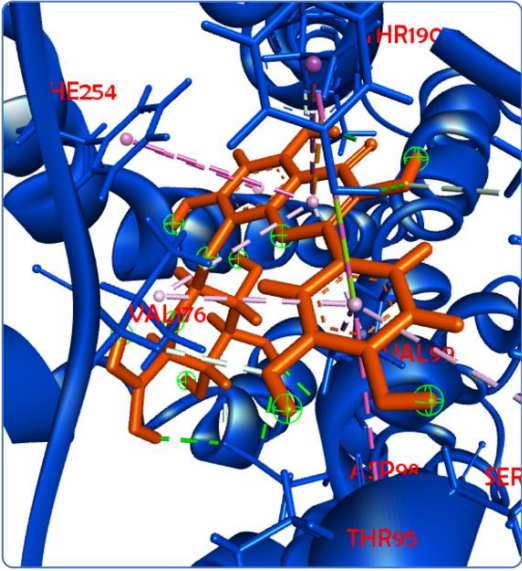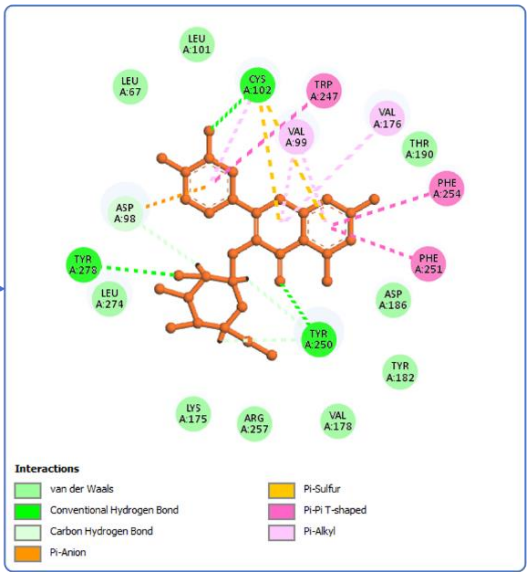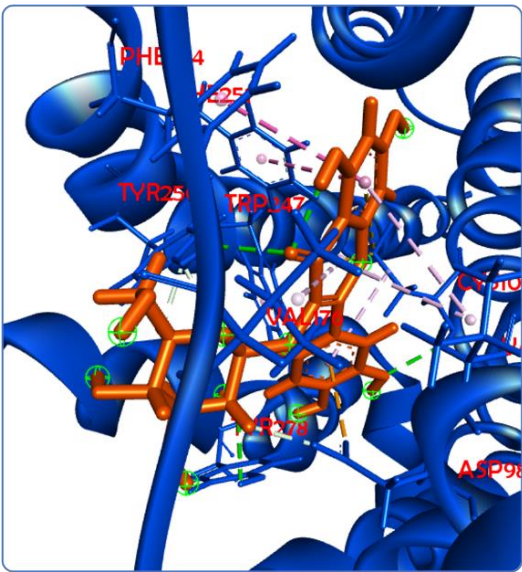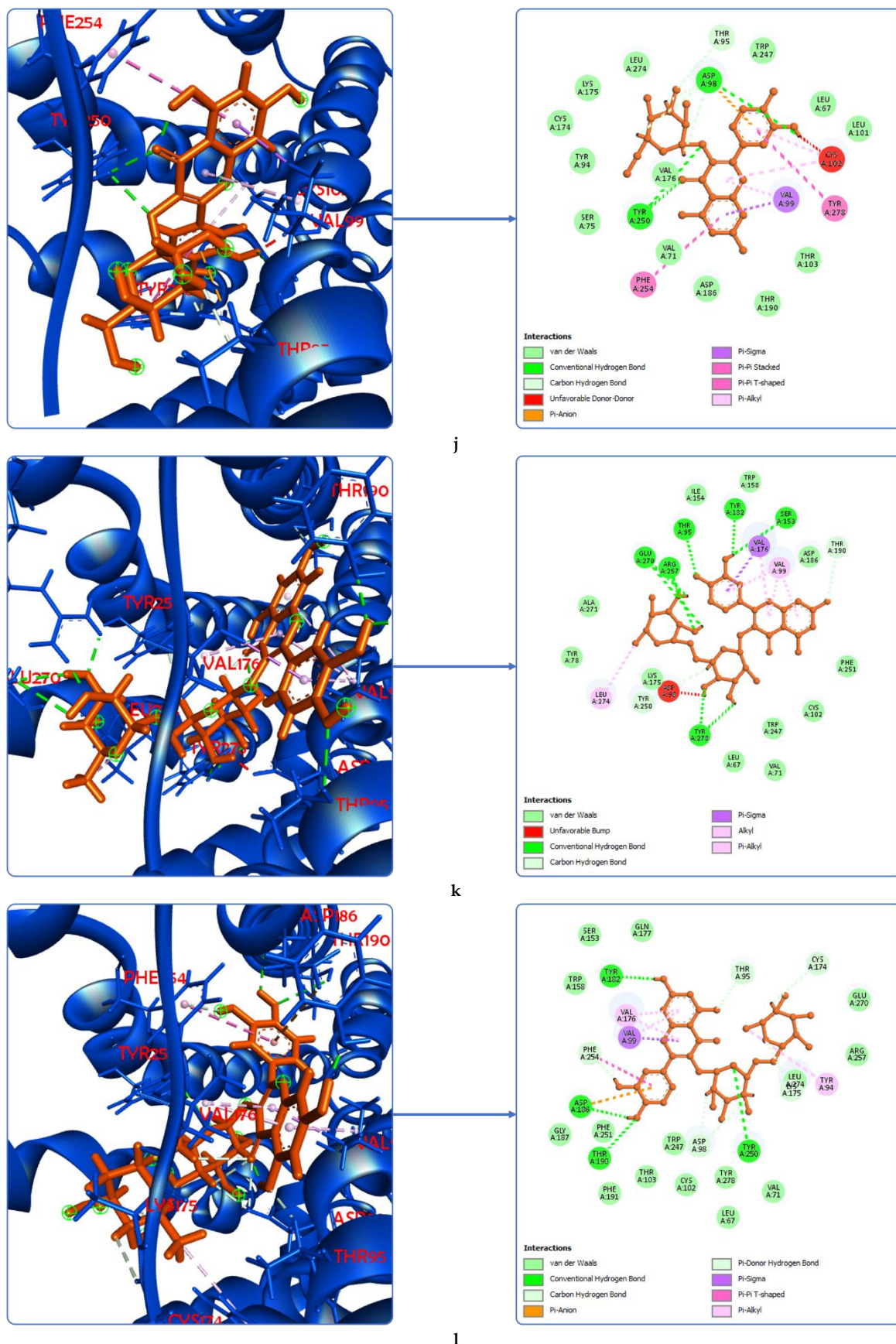
Table III. Ligand binding affinity and key residues.

Ligands	Binding affinity (kcal/mol)	Asp98 (Å)	Asp186 (Å)	Val99 (Å)	Phe254 (Å)
Native ligand	-6.82	[1] 2.82; [11] 5.00	[5]	[6] 4.17	-
Ranitidine	-6.22	[2] 2.76; 2.62; 2.14	[5]	-	-
Quercetin	-6.92	[3] 2.85	[5]	[6] 4.24; 4.87	-
Myricetin	-5.44	[3] 4.61	[5]	[6] 4.40; 5.07	[6] 5.22; [8] 5.40
Myricetin 3-O-glucoside	-2.23	[2] 2.18; [3] 3.13	[5]	[6] 4.50	[8] 4.83
Myricetin 3′-O-glucoside	-5.3	[3] 2.95	[5]	[2] 2.18; [6] 4.55; 5.12	[8] 5.16; [9] 2.59
Hibifolin	-10.47	[1] 1.58; [2] 2.17; 2.46; 2.90; [3] 3.61	[5]	[6] 4.57	[8] 4.79
Isoquercetin	-4.81	[1] 2.42; 2.50; 2.87; [2] 1.90	[3] 3.14	[6] 4.29; [7] 2.65	[10] 4.37; 5.74
Hyperoside	-2.86	[2] 2.21; [3] 2.95	[5]	[6] 4.29; 5.14	[8] 5.03
Quercetin 3′-O-glucoside	-1.49	[1] 2.99; [2] 1.83; 2.62; [3] 3.68	[5]	[6] 4.42; [7] 2.92	[8] 5.76
Quercetin 3-O-robinobioside	-4.89	[4] 1.58	[5]	[7] 2.61	-
Rutin	-2.46	[2] 2.34; 2.60	[1] 2.21	[6] 4.33; [7] 2.61	[8] 5.22

Note: [1] conventional hydrogen; [2] carbon-hydrogen.; [3] π-anion; [4] steric bump; [5] van der waals; [6] π-alkyl; [7] π-sigma; [8] π-π t-shaped; [9] π-donor-hydrogen; [10] π-π stacked; [11] attractive charge.

The initial evaluation of the molecular docking results is primarily based on the binding affinity value. A lower binding affinity indicates that more energy is released upon forming the bond, which, in turn, suggests that a greater amount of energy is required to break it. This strong bond signifies a more stable and favorable interaction between the ligand and the receptor[32]. Following this, the specific types of bonds formed are examined, as each bond type possesses a different interaction strength. Finally, the bond distance and the number of interactions are assessed to provide a more detailed understanding of the binding quality. A shorter bond distance generally correlates with a stronger bond[33]. Similarly, a greater number of interactions, assuming the same bond type, indicates a stronger and more comprehensive binding to the receptor[34]. For instance, if a ligand like quercetin forms multiple interactions, such as two π-alkyl interactions with a residue like Val199, this multiplicity suggests a more robust and stable complex[35].

Based on the physicochemical and pharmacokinetic analyses in **Tables I** and **II**, and the molecular docking results in **Table III**, a comprehensive summary is provided in **Table IV**, leading to the conclusion that quercetin and myricetin are the most potent ligands as H_2 receptor antagonists. Between the two, quercetin stands out as the most promising candidate due to its favorable physicochemical and pharmacokinetic profile, combined with a superior binding affinity that is lower than the positive control. Quercetin and myricetin both form crucial interactions with key residues in the H_2 receptor binding site; however, it's worth noting that quercetin exhibits a unique interaction by binding to the hydrophobic residue Val99. Other ligands tested were deemed less suitable, primarily because they failed to meet the necessary Lipinski's rule of five criteria and demonstrated lower binding affinities compared to the positive control. For instance, while quercetin-O-glucoside had the lowest affinity, it was disqualified as a potential drug candidate due to its unfavorable physicochemical properties and predicted toxicity. Despite its relatively low concentration in *A. manihot* flowers, ranking tenth among the flavonoids at approximately 185.95 µg/g[5], quercetin's superior physicochemical-pharmacokinetic properties and strong molecular potential as an H_2 receptor antagonist highlight its therapeutic significance. The findings from this *in silico* study provide a robust foundation for further pharmacological investigations into the potential of *A. manihot* flowers as a natural source for anti-ulcer treatments.

Table IV. Analysis summary.

Ligands	Lipinski's rule of five	ADMET					Molecular docking
		Absorption	Distribution	Metabolism	Elimination	Toxicity	
Ranitidine	Yes	1st	3rd	Good	1st	Non-toxic	4th
Quercetin	Yes	2nd	2nd	Good	5th	Non-toxic	3rd
Myricetin	Yes	3rd	6th	Good	3rd	Non-toxic	6th
Myricetin 3-O-glucoside	No	5th	1st	Good	8th	Toxic	10th
Myricetin 3′-O-glucoside	No	5th	4th	Good	7th	Toxic	9th
Hibifolin	No	7th	7th	Good	4th	Non-toxic	2nd
Isoquercetin	No	4th	8th	Good	2nd	Toxic	8th
Hyperoside	No	4th	8th	Good	2nd	Toxic	7th
Quercetin 3′-O-glucoside	No	4th	5th	Good	9th	Toxic	1st
Quercetin 3-O-robinobioside	No	6th	9th	Good	6th	Toxic	11th
Rutin	No	6th	9th	Good	6th	Toxic	5th

Note: The serial number indicates the order of the best ligands in each criterion; the smaller the number, the better the test ligand.

CONCLUSION

Based on the *in silico* analysis, quercetin emerges as the most promising flavonoid compound from *A. manihot* flowers for its potential H_2 receptor antagonist activity. This conclusion is supported by several key findings: quercetin meets the necessary physicochemical and pharmacokinetic criteria, suggesting good oral bioavailability. Furthermore, it exhibits a strong binding affinity to the H_2 receptor, with a docking score of -6.92 kcal/mol, which is superior to both the native ranitidine ligand (-6.82 kcal/mol) and the ranitidine control ligand (-6.22 kcal/mol). The compound also forms crucial interactions with key amino acid residues known to be vital for H_2 receptor antagonism. Although the quantitative content of quercetin in the plant may be relatively low, these findings collectively indicate that the potential of *A. manihot* flowers as an anti-gastritis agent is significant and warrants further investigation. Therefore, this study provides a strong rationale for exploring the therapeutic use of *A. manihot* flowers as a natural source of H_2 receptor antagonists.

ACKNOWLEDGMENT

AUTHORS' CONTRIBUTION

Conceptualization: Yuanita Amalia Hariyanto, Trina Ekawati Tallei, Elly Juliana Suoth, Sri Sudewi, Fatimawali
Data curation: Gregorius Giani Adikila
Formal analysis: Gregorius Giani Adikila
Funding acquisition: -
Investigation: Gregorius Giani Adikila
Methodology: Yuanita Amalia Hariyanto, Trina Ekawati Tallei, Elly Juliana Suoth, Sri Sudewi, Fatimawali
Project administration: Fatimawali
Resources: -
Software: Trina Ekawati Tallei, Fatimawali
Supervision: Trina Ekawati Tallei, Elly Juliana Suoth, Sri Sudewi, Fatimawali
Validation: Trina Ekawati Tallei, Elly Juliana Suoth, Sri Sudewi, Fatimawali
Visualization: -
Writing - original draft: Gregorius Giani Adikila
Writing - review & editing: Gregorius Giani Adikila, Yuanita Amalia Hariyanto

DATA AVAILABILITY

None.

CONFLICT OF INTEREST

The authors declare no conflicts of interest related to this study.

REFERENCES

1. Wang L, Jiang W, Li H. Global, regional, and national burden of gastritis and duodenitis from 1990 to 2021 with projections to 2050: a systematic analysis of the Global Burden of Disease Study 2021. Int J Med Sci. 2025;22(11):2570-82. DOI: 10.7150/ijms.109762; PMCID: PMC12163426; PMID: 40520897

2. Talukder A, Kelly M, Gray D, Sarma H. Prevalence and trends of double burden of malnutrition at household-level in South and Southeast Asia. Discov Public Health. 2024;21:212. DOI: 10.1186/s12982-024-00339-y

3. Mandey JS, Sompie FN, Rustandi, Pontoh CJ. Effects of Gedi Leaves (Abelmoschus manihot (L.) Medik) as a Herbal Plant Rich in Mucilages on Blood Lipid Profiles and Carcass Quality of Broiler Chickens as Functional Food. Proced Food Sci. 2015;3:132-6. DOI: 10.1016/j.profoo.2015.01.013

4. Zhang J, Fu ZL, Chu ZX, Song BW. Gastroprotective Activity of the Total Flavones from Abelmoschus manihot (L.) Medic Flowers. Evid Based Complement Alternat Med. 2020;2020:e6584945. DOI: 10.1155/2020/6584945; PMCID: PMC7060849; PMID: 32184895

5. Yin S, Mei Y, Wei L, Zou L, Cai Z, Wu N, et al. Comparison of Multiple Bioactive Constituents in the Corolla and Other Parts of Abelmoschus manihot. Molecules. 2021;26(7):1864. DOI: 10.3390/molecules26071864; PMCID: PMC8037085; PMID: 33806187

6. Zhang W, Lian Y, Li Q, Sun L, Chen R, Lai X, et al. Preventative and Therapeutic Potential of Flavonoids in Peptic Ulcers. Molecules. 2020;25(20):4626. DOI: 10.3390/molecules25204626; PMCID: PMC7594042; PMID: 33050668

7. Serafim C, Araruna ME, Júnior EA, Diniz M, Hiruma-Lima C, Batista L. A Review of the Role of Flavonoids in Peptic Ulcer (2010–2020). Molecules. 2020;25(22):5431. DOI: 10.3390/molecules25225431; PMCID: PMC7699562; PMID: 33233494

8. Garg G. Antiulcer Agents. Edited Book of Pharmacology-III [According to Latest Syllabus of B Pharm-VI Semester of Pharmacy Council of India]. Chikkamagaluru: Iterative International Publishers; 2024. DOI: 10.58532/nbennurphch2

9. Tam PK, Saing H. The use of H2-receptor antagonist in the treatment of peptic ulcer disease in children. J Pediatr Gastroenterol Nutr. 1989;8(1):41-6. DOI: 10.1097/00005176-198901000-00009; PMID: 2567346

10. Pathak R, Chandra P. Bioactive Compounds from Myrica esculenta: Antioxidant Insights and Docking Studies on H+K+-ATPase and H2 Receptor Targets. Med Chem. 2025;21. DOI: 10.2174/0115734064366819250125070619; PMID: 39917935

11. Pratama MRF, Poerwono H, Siswodiharjo S. ADMET properties of novel 5-O-benzoylpinostrobin derivatives. J Basic Clin Physiol Pharmacol. 2019;30(6):20190251. DOI: 10.1515/jbcpp-2019-0251; PMID: 31851612

12. Zhang J, Qi T, Wei J. Homology Modeling and Antagonist Binding Site Study of the Human Histamine H2 Receptor. Med Chem. 2012;8(6):1084–92. DOI: 10.2174/1573406411208061084; PMID: 22779803

13. Chagas CM, Moss S, Alisaraie L. Drug metabolites and their effects on the development of adverse reactions: Revisiting Lipinski's Rule of Five. Int J Pham. 2018;549(1-2):133–49. DOI: 10.1016/j.ijpharm.2018.07.046; PMID: 30040971

14. Lipinski CA, Lombardo F, Dominy BW, Feeney PJ. Experimental and computational approaches to estimate solubility and permeability in drug discovery and development settings. Adv Drug Deliv Rev. 2001;46(1-3):3–26. DOI: 10.1016/s0169-409x(00)00129-0; PMID: 11259830

15. Kumari L, Choudhari Y, Patel P, Gupta GD, Singh D, Rosenholm JM, et al. Advancement in Solubilization Approaches: A Step towards Bioavailability Enhancement of Poorly Soluble Drugs. Life. 2023;13(5):1099. DOI: 10.3390/life13051099; PMCID: PMC10221903; PMID: 37240744

16. Arora D, Khurana B. Computer-Aided Biopharmaceutical Characterization: Gastrointestinal Absorption Simulation and In Silico Computational Modeling. In: Saharan VA, editor. Computer Aided Pharmaceutics and Drug Delivery. Singapore: Springer; 2022. DOI: 10.1007/978-981-16-5180-9_7

17. Prachayasittikul V, Prachayasittikul V. P-glycoprotein transporter in drug development. EXCLI J. 2016;15:113–8. DOI: 10.17179/excli2015-768; PMCID: PMC4817426; PMID: 27047321

18. Holt K, Nagar S, Korzekwa K. Methods to Predict Volume of Distribution. Curr Pharmacol Rep. 2019;5(5):391-9. DOI: 10.1007/s40495-019-00186-5; PMCID: PMC8221585; PMID: 34168949

19. del Amo EM, Ghemtio L, Xhaard H, Yliperttula M, Urtti A, Kidron H. Correction: Applying Linear and Non-Linear Methods for Parallel Prediction of Volume of Distribution and Fraction of Unbound Drug. PLoS One. 2015;10(10):e0141943. DOI: 10.1371/journal.pone.0141943; PMCID: PMC4624968; PMID: 26509808

20. Zhao M, Ma J, Li M, Zhang Y, Jiang B, Zhao X, et al. Cytochrome P450 Enzymes and Drug Metabolism in Humans. Int J Mol Sci. 2021;22(23):12808. DOI: 10.3390/ijms222312808; PMCID: PMC8657965; PMID: 34884615

21. Hakkola J, Hukkanen J, Turpeinen M, Pelkonen O. Inhibition and induction of CYP enzymes in humans: an update. Arch Toxicol. 2020;94(11):3671–722. DOI: 10.1007/s00204-020-02936-7; PMCID: PMC7603454; PMID: 33111191

22. Borra SS, Jane NR, Palaniappan D, Subramanian R, Patankar MA, Krishnamoorthy SG, et al. Genetic polymorphism of organic cation transporter 2 (OCT2) and its effects on the pharmacokinetics and pharmacodynamics of Metformin: a narrative review. Egypt J Med Hum Genet. 2023;24:13. DOI: 10.1186/s43042-023-00388-z

23. Iwata H, Matsuo T, Mamada H, Motomura T, Matsushita M, Fujiwara T, et al. Predicting Total Drug Clearance and Volumes of Distribution Using the Machine Learning-Mediated Multimodal Method through the Imputation of Various Nonclinical Data. J Chem Inf Model. 2022;62(17):4057-65. DOI: 10.1021/acs.jcim.2c00318; PMCID: PMC9472274; PMID: 35993595

24. Amorim AMB, Piochi LF, Gaspar AT, Preto AJ, Rosário-Ferreira N, Moreira IS. Advancing Drug Safety in Drug Development: Bridging Computational Predictions for Enhanced Toxicity Prediction. Chem Res Toxicol. 2024;37(6):827-49. DOI: 10.1021/acs.chemrestox.3c00352; PMCID: PMC11187637; PMID: 38758610

25. Bell EW, Zhang Y. DockRMSD: an open-source tool for atom mapping and RMSD calculation of symmetric molecules through graph isomorphism. J Cheminform. 2019;11(1):40. DOI: 10.1186/s13321-019-0362-7; PMCID: PMC6556049; PMID: 31175455

26. Pratama MRF, Poerwono H, Siswodihardjo S. Molecular docking of novel 5-O-benzoylpinostrobin derivatives as wild type and L858R/T790M/V948R mutant EGFR inhibitor. J Basic Clin Physiol Pharmacol. 2019;30(6):20190301. DOI: 10.1515/jbcpp-2019-0301; PMID: 31855568

27. Kržan M, Keuschler J, Mavri J, Vianello R. Relevance of Hydrogen Bonds for the Histamine H2 Receptor-Ligand Interactions: A Lesson from Deuteration. Biomolecules. 2020;10(2):196. DOI: 10.3390/biom10020196

28. Cao J, Li F, Xia W, Bian W. van der Waals interactions in bimolecular reactions. Chin J Chem Phys. 2019;32(2):157–66. DOI: 10.1063/1674-0068/cjcp1901007

29. Adhav VA, Saikrishnan K. The Realm of Unconventional Noncovalent Interactions in Proteins: Their Significance in Structure and Function. ACS Omega. 2023;8(25):22268-84. DOI: 10.1021/acsomega.3c00205; PMCID: PMC10308531; PMID: 37396257

30. Panwaria P, Das A. Understanding the $n \rightarrow \pi^*$ non-covalent interaction using different experimental and theoretical approaches. Phys Chem Chem Phys. 2022;24(37):22371-89. DOI: 10.1039/D2CP02070J

31. Kirsch P, Hartman AM, Hirsch AKH, Empting M. Concepts and Core Principles of Fragment-Based Drug Design. Molecules. 2019;24(23):4309. DOI: 10.3390/molecules24234309; PMCID: PMC6930586; PMID: 31779114

32. Lang PF. Bond order and bond energies. Found Chem. 2024;26:167–77. DOI: 10.1007/s10698-023-09486-7

33. Chourasia M, Cowen T, Friedman-Ezra A, Rubanovich E, Shurki A. The effect of immediate environment on bond strength of different bond types—A valence bond study. J Chem Phys. 2022;157(24):244301. DOI: 10.1063/5.0130020; PMID: 36586970

34. Buchwald P. A Receptor Model With Binding Affinity, Activation Efficacy, and Signal Amplification Parameters for Complex Fractional Response Versus Occupancy Data. Front Pharmacol. 2019;10:605. DOI: 10.3389/fphar.2019.00605; PMCID: PMC6580154; PMID: 31244653

35. Zhao L, Zhi M, Frenking G. The strength of a chemical bond. Int J Quantum Chem. 2022;122(8):e26773. DOI: 10.1002/qua.26773